SGLT2 Deletion Improves Glucose Homeostasis and Preserves Pancreatic β-Cell Function

Michael J. Jurczak,[1] Hui-Young Lee,[1] Andreas L. Birkenfeld,[2] Francois R. Jornayvaz,[2] David W. Frederick,[2] Rebecca L. Pongratz,[2] Xiaoxian Zhao,[2] Gilbert W. Moeckel,[3] Varman T. Samuel,[2] Jean M. Whaley,[4] Gerald I. Shulman,[1,2,5] and Richard G. Kibbey[2,5]

OBJECTIVE—Inhibition of the Na^+-glucose cotransporter type 2 (SGLT2) is currently being pursued as an insulin-independent treatment for diabetes; however, the behavioral and metabolic consequences of SGLT2 deletion are unknown. Here, we used a SGLT2 knockout mouse to investigate the effect of increased renal glucose excretion on glucose homeostasis, insulin sensitivity, and pancreatic β-cell function.

RESEARCH DESIGN AND METHODS—SGLT2 knockout mice were fed regular chow or a high-fat diet (HFD) for 4 weeks, or backcrossed onto the *db/db* background. The analysis used metabolic cages, glucose tolerance tests, euglycemic and hyperglycemic clamps, as well as isolated islet and perifusion studies.

RESULTS—SGLT2 deletion resulted in a threefold increase in urine output and a 500-fold increase in glucosuria, as well as compensatory increases in feeding, drinking, and activity. SGLT2 knockout mice were protected from HFD-induced hyperglycemia and glucose intolerance and had reduced plasma insulin concentrations compared with controls. On the *db/db* background, SGLT2 deletion prevented fasting hyperglycemia, and plasma insulin levels were also dramatically improved. Strikingly, prevention of hyperglycemia by SGLT2 knockout in *db/db* mice preserved pancreatic β-cell function in vivo, which was associated with a 60% increase in β-cell mass and reduced incidence of β-cell death.

CONCLUSIONS—Prevention of renal glucose reabsorption by SGLT2 deletion reduced HFD- and obesity-associated hyperglycemia, improved glucose intolerance, and increased glucose-stimulated insulin secretion in vivo. Taken together, these data support SGLT2 inhibition as a viable insulin-independent treatment of type 2 diabetes. *Diabetes* 60:890–898, 2011

Treatments of type 2 diabetes must balance the prevention of microvascular complications with the minimization of clinically significant hypoglycemia. The difficulty in safely achieving these goals, combined with epidemic increases in diabetes worldwide, has spurred the search for novel therapeutic strategies. Among these, inhibition of the Na^+-glucose cotransporter type 2 (SGLT2) has emerged as a promising therapy (1,2). SGLT2 is a member of the *SLC5* gene family and transports glucose across cells using the Na^+ gradient established by Na^+-K^+-ATPases (3). SGLT2 is a low-affinity, high-capacity transporter expressed predominantly in the early proximal tubule of the kidney and accounts for about 90% of renal glucose reabsorption (4–6). Given that the kidney filters approximately 180 g of glucose daily, SGLT2 inhibition may not just reduce hyperglycemia but may also promote negative energy balance and weight loss.

Type 2 diabetes is characterized by fasting hyperglycemia as a result of insulin resistance, but is often preceded by hyperinsulinemia and normal blood glucose levels, a state that is maintained by compensatory insulin secretion by the pancreatic β-cell (7). The ability of the β-cell to counteract an increased glucose load is short-lived, however, and eventually pancreatic islets fail, giving rise to hyperglycemia. Rodent and human studies have both shown that glucose toxicity is implicated in β-cell failure by increasing the rate of β-cell death by the induction of proapoptotic genes (8–10). Inhibition of SGLT2 therefore has the potential to not only acutely lower hyperglycemia but to also improve glucose homeostasis by reducing glucose toxicity and preventing islet failure.

Despite recent interest in SGLT2 as a potential target for diabetes treatment, relatively few long-term models of SGLT2 deficiency have been characterized. Previously, nonselective inhibition of both SGLT1 and SGLT2 for 4 weeks in partially pancreatomized diabetic rats by injection of phlorizin led to increases in insulin sensitivity and insulin secretion (11,12). More recently, improvements in glucose homeostasis were demonstrated in diabetic rodent models after treatment with SGLT2-specific inhibitors for periods of 2 to 9 weeks (13–16). As many as seven different SGLT2 inhibitors designed for use in humans have been characterized in cell culture and animal studies, and many of these have moved on to clinical trials (2,17–22). Here, we describe the first in vivo characterization of glucose homeostasis in a SGLT2 knockout mouse model. We investigated the behavioral and metabolic consequences of SGLT2 deletion, and furthermore, we determined the effect of renal glucose excretion on glucose homeostasis, insulin sensitivity, and β-cell function in the context of both high-fat feeding and genetically determined obesity (*db/db*) and diabetes.

RESEARCH DESIGN AND METHODS

Animals and diets. The SGLT2 (*Slc5a2*) deficient mice were generated by Lexicon Pharmaceuticals, Inc. (The Woodlands, TX) as previously described (6). SGLT2 and *db/db* backcrosses were performed at The Jackson Laboratory (Bar Harbor, ME) and shipped to Yale for studies. Mice were housed at Yale

University School of Medicine and maintained in accordance with the Institutional Animal Care and Use Committee guidelines. Mice were housed at $22 \pm 2°C$ on a 12-h light/dark cycle with free access to food and water. Mice were fed regular chow (RC; 18% fat, 58% carbohydrate, 24% protein by calories; TD2018; Harlan Teklad, Madison, WI) or 4 weeks of high-fat diet (HFD; 55% fat, 24% carbohydrate, 21% protein by calories; TD93075; Harlan Teklad).

Body composition was determined by ^1H magnetic resonance spectroscopy (Bruker Minispec). The Comprehensive Laboratory Animal Monitoring System (Columbus Instruments, Columbus, OH) was used to evaluate activity, energy expenditure, feeding, drinking, and respiratory quotient over the course of 48 h. Data are the 24-h average normalized to body weight. For the urine collection studies, mice were housed for 24 h with free access to food and water in wire-bottomed cages designed to separate and collect urine and feces.

In vivo glucose homeostasis. Glucose tolerance tests were performed after an overnight fast. Mice were injected intraperitoneally with 1 mg/kg glucose, and blood was collected by tail bleed at set times for plasma insulin and glucose measurements. Hyperinsulinemic euglycemic clamps were performed as previously described (23), with minor modifications. Specifically, clamp duration was extended to 180 min and the insulin dose was increased to $20 \text{ mU} \cdot \text{kg}^{-1} \cdot \text{min}^{-1}$. Hyperglycemic clamps were conducted after an overnight fast. Mice were given a primed/variable infusion of glucose to reach and maintain hyperglycemia during the 120-min experiment. Blood was collected at set intervals by tail bleeds for determination of plasma glucose and insulin. Because of differences in fasting plasma glucose and insulin levels between genotypes, infusion rates were chosen to achieve matched changes in plasma glucose (Δ glucose), and the change in plasma insulin from baseline (Δ insulin) was used to assess the pancreatic β-cell response.

Pancreas and islet studies. Isolated islet studies were conducted as previously described (24). In brief, pancreata were removed from anesthetized mice and minced in CMRL media with type P collagenase to disperse cells. Islets were hand picked under a light microscope and allowed to recover overnight in media. Eighty islets were picked and loaded into a perifusion chamber with acrylamide gel column beads (Bio-Gel P4G; Bio-Rad, Hercules, CA) and perfusion buffer (Krebs-Ringer buffer with 3 mmol/L glucose and 0.2% fatty acid-free BSA). Perifusions were conducted with a Bio-Rep (Miami, FL) perifusion instrument that allows for precise temperature and flow control and collection of samples into 96-well format. After a 1-h equilibration period, islets were perifused with the indicated agonists, and samples were collected at 1-min intervals for 40 min. At the end of the perifusion, islet DNA was isolated and quantified for normalization of insulin and glucagon data using a Picogreen dsDNA quantitation kit (Invitrogen) according to the manufacturer's instructions.

Preparation and staining of all histologic samples were conducted at the Department of Pathology Histology Core at Yale. Samples were fixed in 4% formalin overnight and set in paraffin wax. Sections were cut at 5 μm, dried, deparaffinized, and rehydrated with distilled water. For kidney studies, hematoxylin and eosin (H&E) stains were analyzed in a blinded fashion by a pathologist. For pancreas studies, transferase-mediated dUTP nick-end labeling (TUNEL) reaction was performed according to the manufacturer's instructions (Millipore S7100; Millipore, Billerica, MA), after which slides were incubated with polyclonal anti-insulin (Dako 0564) and visualized by an alkaline-phosphatase–based method (Dako K5355).

Frequency of cell death was calculated as the number of insulin/TUNEL-positive cells corrected by relative islet area (islet area/pancreas area) for 10 to 15 fields per section and three sections per mouse. Islet number was determined by counting all islets within a given field, corrected to pancreas area. Approximately 30 fields were taken at random, and three sections per mouse were analyzed. Sections were staggered to reduce the possibility of analyzing the same islet twice. For proliferation studies, slides were incubated with anti-Ki-67 (Biocare Medical CRM325) and anti-insulin (Dako A0564) and visualized with peroxidase and fluorescent secondary antibodies (Dako K4003, Invitrogen A11073). Frequency of cellular proliferation was calculated in a similar fashion as frequency of cell death. Pancreas weights were not available, so relative β-cell volume was calculated as the ratio of islet area/pancreas area. Cell size measurements were made using ImageJ software.

Biochemical analyses. Plasma and urine glucose concentrations were measured by a glucose oxidase method using a Beckman Glucose Analyzer II. Plasma insulin was measured by radioimmunoassay kit (Linco Research, St. Louis, MO), and fatty acids were measured by a spectrophotometric technique (Wako NEFA Kit, Osaka, Japan). Hepatic glycogen content was measured as previously described, except that a 10:1 volume/weight dilution was used for homogenization (25). Insulin and glucagon from isolated islets were measured with the LINCOplex platform (Millipore). Plasma chemistries were measured with a Roche COBAS Mira automated chemistry analyzer at the Yale Mouse Metabolic Phenotyping Center Analytical Core. Plasma creatinine levels were determined by high-performance liquid chromatography/mass spectrometry/mass spectrometry.

Statistical analysis. Data are reported as the mean $\pm$ SEM. Comparisons between groups were made using unpaired, two-tailed Student t tests. For time course data, two-way and one-way ANOVA were used where appropriate. A value of $P < 0.05$ was considered significant. Statistical analyses were performed using GraphPad Prism 5 software.

RESULTS

Phenotype of SGLT2$^{-/-}$ RC- and HFD-fed mice. The RC-fed SGLT2$^{-/-}$ mice weighed approximately 10% less than wild-type (WT) mice at age 16 weeks (Table 1). To determine the effect of SGLT2 deletion in the presence of increased body weight and adiposity, a second group of SGLT2$^{-/-}$ and WT mice were fed an HFD for 4 weeks. HFD mice had an increased body weight compared with controls for both genotypes, but unlike RC-fed mice, HFD/SGLT2$^{-/-}$ mice only trended toward a lower body weight ($P = 0.12$; Table 1). There were no differences in fat mass between RC/WT and RC/SGLT2$^{-/-}$ mice, and HFD/SGLT2$^{-/-}$ animals trended toward reduced adiposity ($P = 0.08$; Table 1).

Daily urine volume was 4.5-fold greater in SGLT2$^{-/-}$ than in WT mice, which translated to a 500-fold increase in glucosuria, with similar findings in the HFD mice (Table 1). Despite increased urine volume and glucosuria, plasma chemistries were unchanged in SGLT2$^{-/-}$ mice (Supplementary Table 1), in agreement with a recently published description of the SGLT2 knockout model (6). There was no difference in the blood urea nitrogen (BUN)/creatinine ratio between WT or SGLT2$^{-/-}$ mice, suggesting that volume depletion could not account for the lower weight (Supplementary Table 1). Histologic analysis of kidney sections revealed normal glomerular structures and tubulointerstitial compartments, without significant histopathologic changes in the proximal or distal nephron of SGLT2$^{-/-}$ mice (Supplementary Fig. 1), and there was no difference in kidney weight between genotypes (Table 1).

TABLE 1
Physiologic overview of SGLT2$^{-/-}$ mice

Mouse	Body weight (g)	Body fat (%)	Kidney weight (mg/g)	Plasma BUN (mg/dL)	Plasma creatinine (mg/dL)	Urine output (mL/day)	Glucosuria (mg/day)
WT	29.4 ± 0.7	6.9 ± 0.7	6.55 ± 0.42	23.2 ± 0.3	0.074 ± 0.001	1.5 ± 0.3	0.9 ± 0.3
SGLT2$^{-/-}$	26.7 ± 0.6*	7.4 ± 0.3	6.49 ± 0.14	23.8 ± 1.1	0.077 ± 0.007	6.7 ± 0.4†	502 ± 30†
HFD/WT	35.0 ± 0.7	26.4 ± 1.2	ND	20.8 ± 0.7	0.103 ± 0.005	1.7 ± 0.2	1.0 ± 0.3
HFD/SGLT2$^{-/-}$	33.0 ± 1.0	22.3 ± 1.9	ND	18.8 ± 0.7	0.119 ± 0.007	5.4 ± 0.5†	431 ± 31†

Data were collected from 16-week-old, ad libitum fed mice. Kidney weight represents the weight of one kidney corrected by body weight. Mice were housed in custom cages for 24 h for urine output and glucosuria measurements. HFD was fed for 4 weeks. $n = 12–16$ per genotype for body weight and fat data; $n = 6–8$ for remaining data. *$P < 0.05$; †$P < 0.001$ for comparison of WT with SGLT2$^{-/-}$ for each diet. Data analyzed by Student t test. ND, not done.

To determine the effect of SGLT2 deletion on whole-body metabolism and behavior, SGLT2$^{-/-}$ and WT mice were housed in metabolic cages. During resting hours (light cycle), there was no difference in activity, energy expenditure, or food intake between genotypes (Supplementary Fig. 2A–C), although water intake was elevated during this time for SGLT2$^{-/-}$ mice (Supplementary Fig. 2D). In contrast, there were marked differences in each parameter between mice during active hours (dark cycle). Activity, energy expenditure, and food and water intake were all significantly increased in SGLT2$^{-/-}$ mice during the dark cycle (Fig. 1A). Notably, there was a 20% increase in feeding and a 190% increase in drinking compared with controls. Despite the increase in caloric intake, SGLT2$^{-/-}$ mice maintained a lower body weight through a combination of 7% higher energy expenditure during the dark cycle and 13% (1.9 kcal/day) caloric loss of carbohydrate in the urine.

Under HFD conditions, mice consume significantly less carbohydrate. Interestingly, unlike RC-fed mice, there were no differences in activity, energy expenditure, or food intake in the light or dark cycle during HFD (Supplementary Fig. 3), consistent with the lower carbohydrate composition of the chow. Drinking, however, was clearly increased relative to HFD controls throughout the day, reflecting continuous glucose loss. In comparison with RC/SGLT2$^{-/-}$ mice, HFD/SGLT2$^{-/-}$ mice had lower water consumption (36.9 ± 2.5 vs. 45.6 ± 2.9 μL/h; $P < 0.05$) and urine output (5.2 ± 0.5 vs. 6.5 ± 0.4 mL/day; $P < 0.05$), again suggesting that carbohydrate content of the chow had a large influence on glucosuria.

The lower respiratory quotient in SGLT2$^{-/-}$ mice (Fig. 1A) reflects a higher rate of lipid relative to carbohydrate oxidation, as might be expected for mice that are carbohydrate-depleted by profound glucosuria. Indeed, there was a 2.5-fold decrease in hepatic glycogen content in SGLT2$^{-/-}$ compared with WT mice (5.1 ± 1.1 vs. 12.7 ± 2.0 μg/mg tissue; $P < 0.05$). This was even more dramatic on the HFD, where the respiratory quotient was 0.78 and approached that of nearly a complete dependence on lipid oxidation (Supplementary Fig. 3E).

Glucose homeostasis is improved in RC- and HFD-fed SGLT2$^{-/-}$ mice. Next, in vivo glucose homeostasis was assessed. Compared with RC/WT mice, RC/SGLT2$^{-/-}$ mice had significantly lower fasting plasma glucose concentrations and a nonsignificant reduction in plasma insulin concentrations (9.0 ± 0.6 and 6.4 ± 1.8 μU/mL insulin; $P = 0.17$; Fig. 1B and C). After 4 weeks of the HFD, fasting glucose was drastically reduced in SGLT$^{-/-}$ compared with WT mice and was indistinguishable from RC/WT controls (Fig. 1B). Plasma insulin concentrations were 50% lower in the HFD/SGLT2$^{-/-}$ compared with WT mice, as would be expected for the lower plasma glucose levels. HFD/SGLT2$^{-/-}$ mice had a twofold increase in fasting insulin compared with RC/WT mice (Fig. 1C), suggesting that SGLT2 deletion did not completely prevent insulin resistance.

Intraperitoneal glucose tolerance tests (IPGTTs) were performed to determine the effect of SGLT2 knockout on glucose homeostasis. Plasma glucose concentrations remained lower in SGLT2$^{-/-}$ than in WT mice for the entire experiment ($P < 0.01$ by two-way ANOVA; Fig. 1D). The area under the curve (AUC) for glucose was 20% lower for SGLT2$^{-/-}$ than for WT mice (Fig. 1F). A similar, but more pronounced effect was observed during HFD studies ($P < 0.001$ by two-way ANOVA; Fig. 1D), where AUC glucose was 40% less in SGLT2$^{-/-}$ mice and was indistinguishable from WT/RC controls (Fig. 1F). Changes in

plasma insulin concentrations roughly mirrored the differences observed for plasma glucose (WT vs. SGLT2$^{-/-}$ RC and HFD $P < 0.01$, two-way ANOVA; Fig. 1E), consistent with appropriate β-cell function. The insulin AUC was 37% less for RC/SGLT2$^{-/-}$ compared with RC/WT mice, while after HFD, the insulin AUC was 53% less for SGLT2$^{-/-}$ mice (Fig. 1G). Thus, loss of SGLT2 significantly improved basal and IPGTT-challenged glucose homeostasis in RC- and HFD-fed mice.

SGLT2 deletion reduces adiposity and improves glucose homeostasis in *db/db* mice. To determine whether loss of SGLT2 was protective in the setting of extreme obesity and insulin resistance, SGLT2$^{-/-}$ mice were bred onto the *db/db* background. The *db/db* mice are leptin receptor–deficient and develop profound hyperphagia, obesity, hypercorticosteronemia, insulin resistance, and eventually, diabetes. At approximately age 18 weeks, body weights were similar for both heterozygous (*db/db*-SGLT2$^{+/-}$) and homozygous (*db/db*-SGLT2$^{-/-}$) SGLT2 deletion compared with controls (*db/db*-SGLT2$^{+/+}$; Fig. 2A), whereas body fat was 5% less in *db/db*-SGLT2$^{-/-}$ mice (Fig. 2B). There was a progressive effect of SGLT2 deletion on urine volume, with *db/db*-SGLT2$^{-/+}$ having a 2.6-fold and *db/db*-SGLT$^{-/-}$ having a fourfold increase (Fig. 2C). The *db/db* mice displayed profound glucosuria, totaling approximately 500 mg/day (Fig. 2D). Still, there was a three- and 4.4-fold increase in *db/db*-SGLT2$^{-/+}$ and *db/db*-SGLT2$^{-/-}$ mice, respectively, indicating that lowering the renal glucose threshold had a progressive effect on glucosuria (Fig. 2D). Astonishingly, total daily glucose loss for *db/db*-SGLT2$^{-/-}$ mice was 2.2 g or 5% of the animals' body weight.

Despite increased glucosuria in *db/db*-SGLT2$^{+/-}$ mice, only the *db/db*-SGLT2$^{-/-}$ mice had significantly reduced plasma glucose concentrations (Fig. 2E). Strikingly, this 75-mg/dL reduction normalized glycemia to the same level as RC/WT mice (WT: 131 ± 6 mg/dL vs. db/db-SGLT2$^{-/-}$: 124 ± 8 mg/dL). Plasma insulin levels were 50% lower in *db/db*-SGLT2$^{-/-}$ crosses (Fig. 2F), consistent with the lower plasma glucose concentration. Plasma insulin levels were 10-fold higher than RC/WT mice (WT: 9.0 ± 0.6 μU/mL vs. *db/db*-SGLT2$^{-/-}$: 112 ± 13 μU/mL), indicating the persistence of insulin resistance in the *db/db* model. Lastly, SGLT2 deletion had no effect on plasma fatty acid levels in *db/db* mice (Fig. 2G).

Euglycemic clamp studies were performed to evaluate the effect of SGLT2 deletion on insulin sensitivity and tissue-specific glucose metabolism. Because of extreme insulin resistance in *db/db* mice, plasma glucose concentrations were clamped at 150 mg/dL using a 20 mU · kg^{-1} · min^{-1} insulin infusion (Supplementary Fig. 4A–D). The glucose infusion rate (GIR) was 2.7-times greater in *db/db*-SGLT2$^{-/-}$ than in *db/db*-SGLT2$^{+/+}$ mice (Table 2). Quantitative measurement of glucosuria during the clamp was not possible for control or *db/db*-SGLT2$^{+/-}$ mice because of small urine volumes, but ranged from 0 to 15% of total GIR for *db/db*-SGLT2$^{-/-}$ mice (data not shown). Thus, the higher GIR could only partially be accounted for by loss as glucosuria and suggested improvements in insulin sensitivity. There was no difference in whole-body or tissue-specific glucose uptake in any group (Table 2), but clamped endogenous glucose production was modestly reduced in *db/db*-SGLT2$^{-/-}$ compared with *db/db*-SGLT2$^{+/+}$ mice (Table 2).

Pancreatic β-cell function is preserved in *db/db*-SGLT2$^{-/-}$ mice. Because glucose toxicity can lead to β-cell failure, we assessed glucose-stimulated insulin secretion
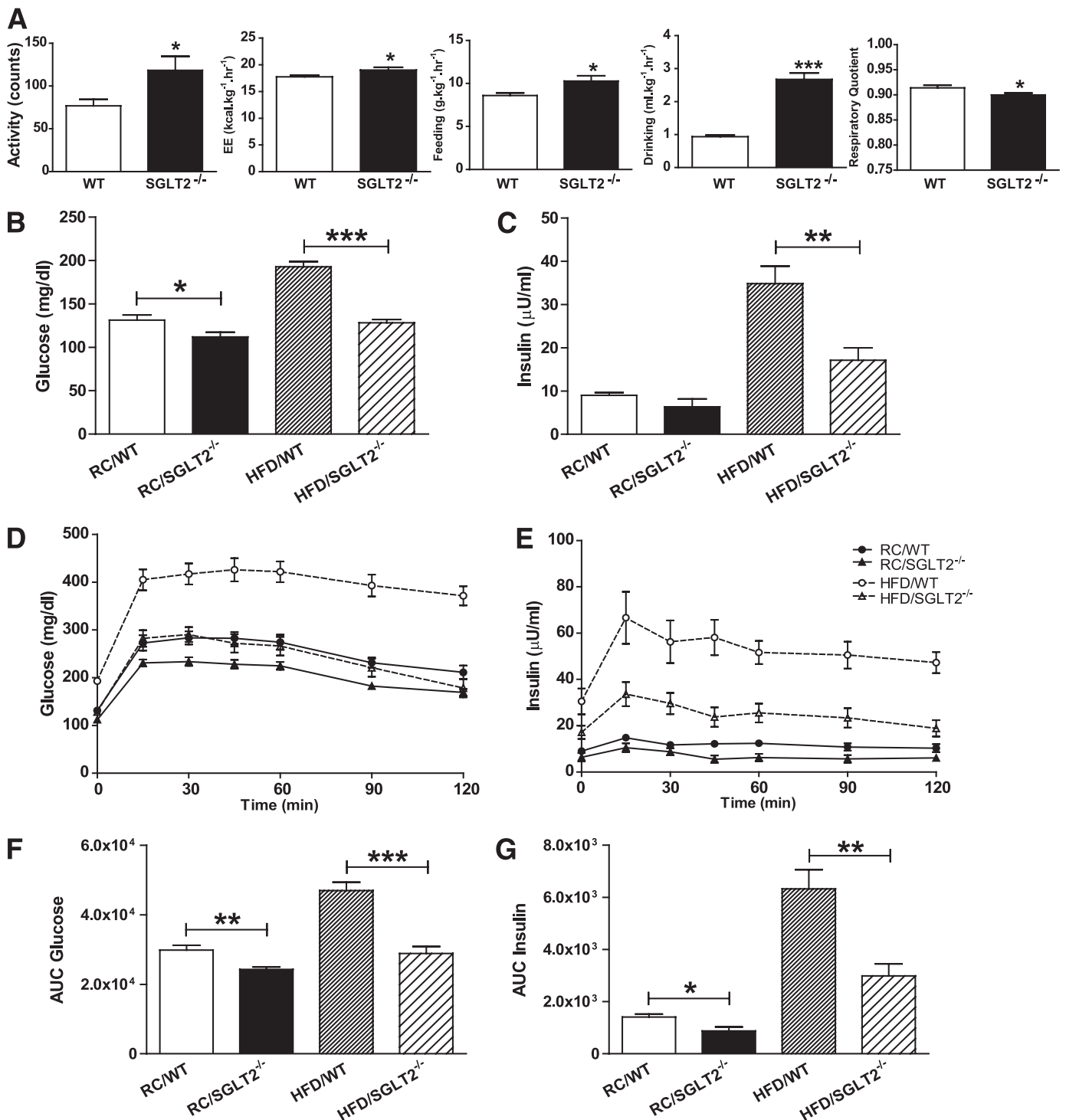
FIG. 1. SGLT2$^{-/-}$ mice are protected from HFD-induced hyperglycemia and glucose intolerance. *A*: Dark cycle averages are shown for metabolic cage data for activity, energy expenditure (EE), feeding, drinking, and respiratory quotient (VCO$_2$/VO$_2$) for WT and SGLT2$^{-/-}$ mice. *B*: Fasting plasma glucose values for RC and HFD WT and SGLT2$^{-/-}$ mice. *C*: Fasting plasma insulin values. *D*: Changes in plasma glucose following intraperitoneal injection of 1-mg/kg glucose (WT vs. SGLT2$^{-/-}$ $P < 0.01$ for RC and $P < 0.001$ for HFD). *E*: Changes in plasma insulin levels during experiment shown in *D* (WT vs. SGLT2$^{-/-}$ $P < 0.01$ for RC and HFD). *F*: AUC for glucose calculated from data in *D*. *G*: AUC for insulin calculated from data in *E*. *n* = 8–12 mice per group. Data were analyzed by unpaired, two-tailed Student *t* test. Significance between curves was determined by two-way ANOVA. *$P < 0.05$, **$P < 0.01$, and ***$P < 0.001$. Data represent the mean ± SEM.

by hyperglycemic clamp. Fasting plasma glucose concentrations varied among genotypes (Fig. 2*E*); therefore, all mice were clamped 200 mg/dL above their basal plasma glucose levels. Similar to euglycemic clamps, the GIR required to maintain hyperglycemia for *db/db*-SGLT2$^{-/-}$ mice was

approximately twofold greater than for controls (Fig. 3*A*). The total increase in plasma glucose concentrations above baseline during the clamp was similar for all three groups (Fig. 3*B* and *C*). No first-phase insulin response was observed, consistent with compromised islet function in *db/db*
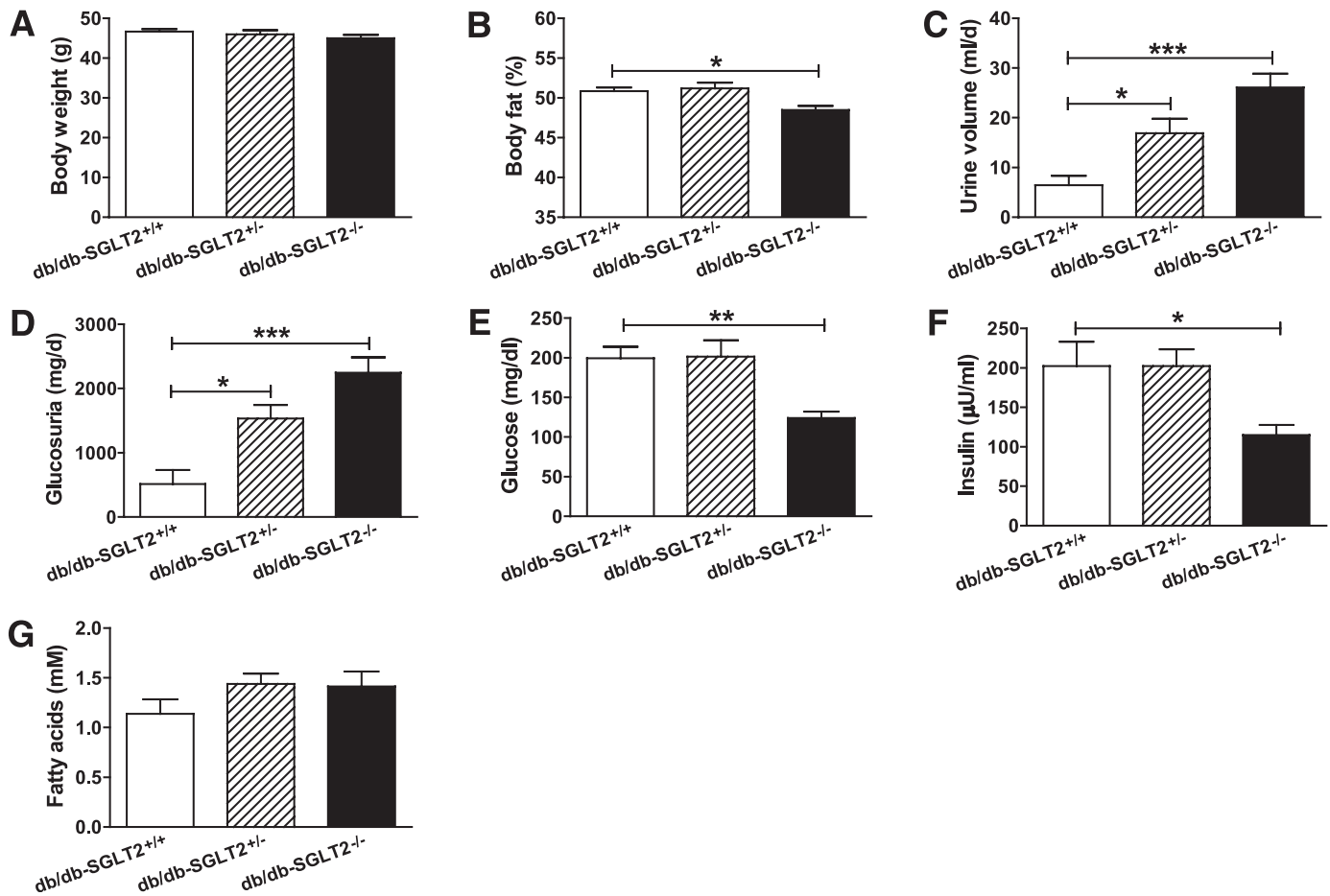
FIG. 2. Increased glucosuria is associated with decreased fasting plasma glucose and insulin in *db/db*-SGLT2$^{-/-}$ mice. *A*: Body weights are shown for *db/db*-SGLT$^{+/+}$, *db/db*-SGLT2$^{+/-}$, and *db/db*-SLGT2$^{-/-}$ mice at approximately 18 weeks of age. *B*: Percentage of body fat determined by proton nuclear magnetic resonance. *C*: Urine volume at 24 h. *D*: Glucosuria at 24 h (*n* = 5–6 per group). *E*: Fasting plasma glucose level. *F*: Insulin levels. *G*: Plasma fatty acid concentrations from overnight fasted mice. *n* = 7–9 per group; *n* = 15–20 per genotype except where noted. Data were analyzed by Student *t* test. *$P < 0.05$, **$P < 0.01$, and ***$P < 0.001$. Data represent the mean ± SEM.

mice (Fig. 3*D*). However, in response to the same net change in plasma glucose concentration (ΔAUC glucose, Fig. 3*C*), *db/db*-SGLT2$^{-/-}$ mice displayed a significant increase in absolute plasma insulin levels during the clamp ($P < 0.001$, one-way ANOVA; Fig. 3*D*), and ΔAUC insulin was 2.4-fold greater compared with *db/db*-SGLT2$^{+/+}$ mice (Fig. 3*E*). Calculation of the change in plasma insulin (Δ insulin) from baseline also demonstrated an approximate twofold increase in glucose-stimulated insulin secretion for *db/db*-SGLT2$^{-/-}$ compared with *db/db*-SGLT2$^{+/+}$ mice (Fig. 3*F*).

Thus, the greater than 10-fold increase in insulin secretion for *db/db*-SGLT2$^{-/-}$ compared with the modest fivefold increase for controls during the hyperglycemic clamp was consistent with improved β-cell function in vivo.

Isolated pancreatic islets from the *db/db*-SGLT2$^{+/+}$ and *db/db*-SGLT2$^{-/-}$ mice were perifused to determine if changes in individual islet function had occurred. During isolation, islet yield was much greater for *db/db*-SGLT2$^{-/-}$ mice, so islets of similar size were selected for comparison. Surprisingly, there was no difference in glucose-stimulated

TABLE 2
Hyperinsulinemic euglycemic clamp studies

Mouse	Plasma glucose (mg/dL)	Glucose infusion rate (mg · kg^{-1} · min^{-1})	Endogenous glucose production (mg · kg^{-1} · min^{-1})	Whole-body glucose uptake (mg · kg^{-1} · min^{-1})	Skeletal muscle glucose uptake (nmol · g^{-1} · min^{-1})	White adipose glucose uptake (nmol · g^{-1} · min^{-1})	Insulin (µU/mL)
db/db							
SGLT2$^{+/+}$	149 ± 13	2.9 ± 0.8	21.3 ± 1.2	24.1 ± 0.9	135 ± 22	24.7 ± 1.8	1211 ± 138
SGLT2$^{+/-}$	152 ± 18	3.9 ± 1.2	19.3 ± 1.9	23.3 ± 1.2	134 ± 18	27.1 ± 2.2	1178 ± 105
SGLT2$^{-/-}$	139 ± 8	8.0 ± 0.8*	16.2 ± 2.1†	24.2 ± 1.9	109 ± 18	25.2 ± 3.4	1268 ± 158

Whole-body and tissue-specific glucose metabolism during hyperinsulinemic infusion. The *db/db*-SGLT2$^{+/+}$ (*n* = 9), *db/db*-SGLT2$^{+/-}$ (*n* = 8), and *db/db*-SGLT2$^{-/-}$ (*n* = 7). Data analyzed by Student *t* test. *$P < 0.01$; †$P < 0.05$ compared with *db/db*-SGLT2$^{+/+}$.
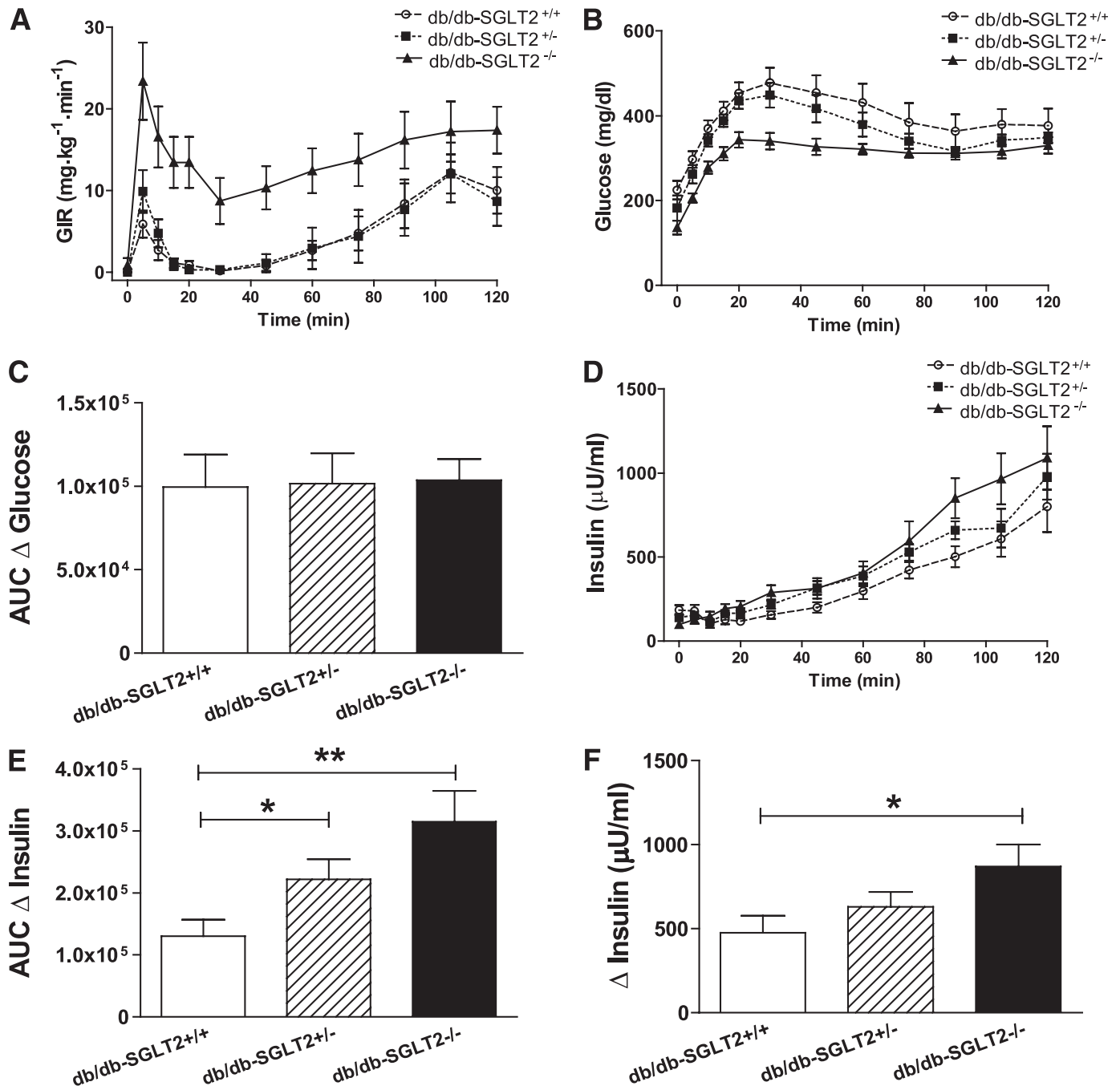
FIG. 3. The *db/db*-SGLT2$^{-/-}$ mice display improved β-cell function in vivo. *A*: Glucose infusion rates (GIR) required to maintain hyperglycemia during 120-min clamp experiment. *B*: Changes in plasma glucose during the clamp in response to GIR in *A*. *C*: AUC calculations are shown for the change in plasma glucose (Δ glucose) from baseline during the clamp. *D*: Changes in plasma insulin in response to changes in plasma glucose in *B* (*db/db*-SGLT2$^{+/+}$ vs. *db/db*-SGLT2$^{-/-}$; *P* < 0.01). *E*: AUC calculation is shown for Δ insulin during glucose stimulation. *F*: Net change in plasma insulin levels from baseline (Δ insulin) during the clamp (*n* = 6–9 per group). Data were analyzed by Student *t* test. Significance between curves was determined by one-way ANOVA. *P* < 0.05, **P* < 0.01. Data represent the mean ± SEM.

insulin secretion (633 ± 104 vs. 743 ± 53 AUC insulin; *P* = 0.37; Fig. 4*A*) or glucagon suppression (0.28 ± 0.12 vs. 0.15 ± 0.04 AUC glucagon; *P* = 0.35; Fig. 4*B*) between groups, suggesting that individual islet function, per se, could not account for the observed in vivo differences. Perifusion studies conducted for WT and SGLT$^{-/-}$ mice on RC and HFD also demonstrated no differences in insulin or glucagon secretion (Supplementary Fig. 5*A–D*).

The difference between hyperglycemic clamp and islet perifusion results suggested that changes in β-cell mass

might account for the increased insulin secretion observed in vivo. Compared with RC/WT mice, relative β-cell volume was increased 3.3- and 5.4-fold for *db/db*-SGLT2$^{+/+}$ and *db/db*-SGLT2$^{-/-}$ mice, respectively, suggesting compensatory hypertrophy as a result of insulin resistance (1.06 ± 0.12, 3.52 ± 0.52, and 5.77 ± 0.21 islet area/pancreas area; *P* < 0.001 by one-way ANOVA). Importantly, there was a 63% increase in relative β-cell volume in *db/db*-SGLT2$^{-/-}$ compared with *db/db*-SGLT2$^{+/+}$ mice (Fig. 4*C* and *G*). The difference in islet mass between *db/db* groups appeared to
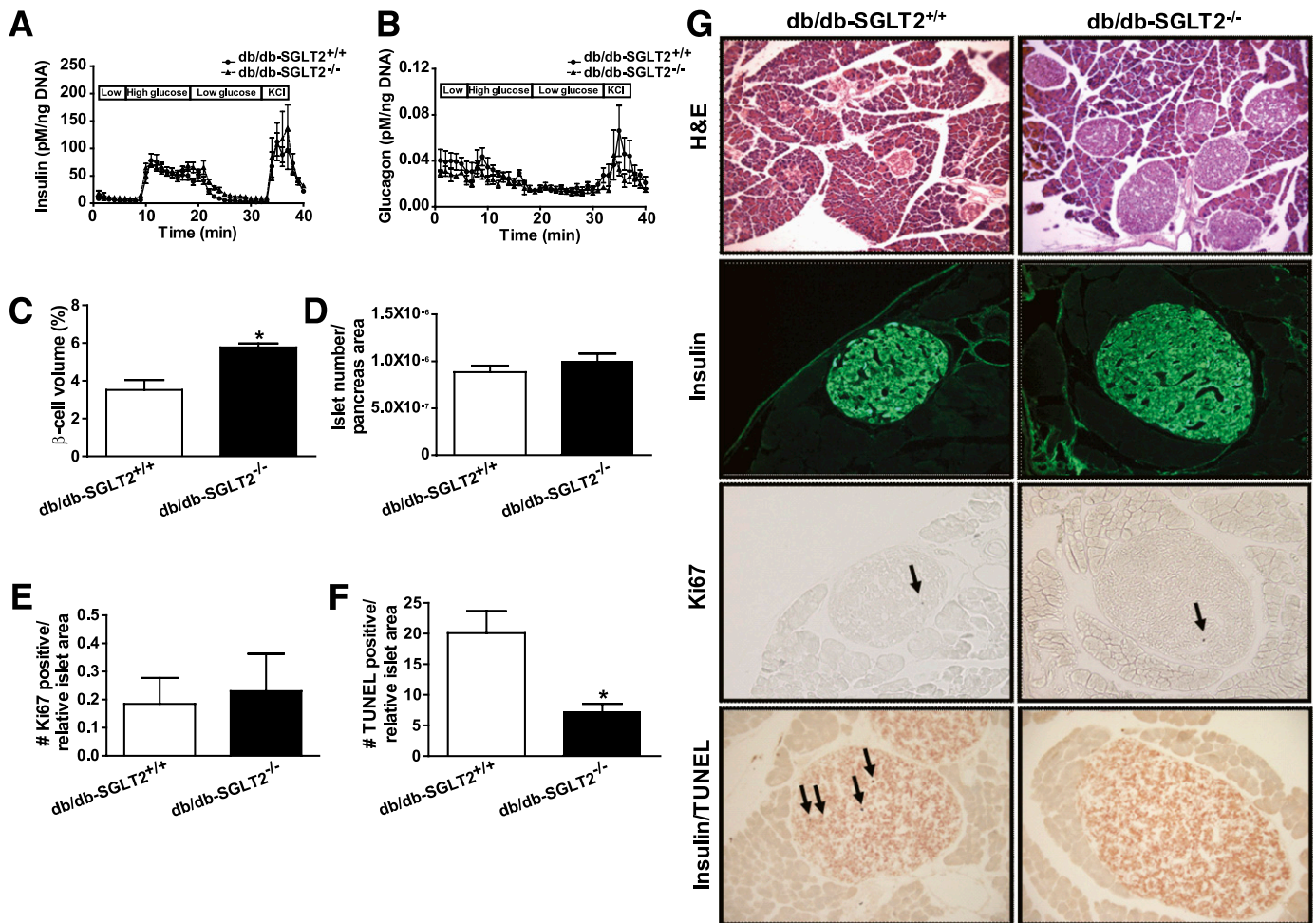
FIG. 4. Pancreatic β-cell mass is increased in *db/db*-SGLT2$^{-/-}$ mice due to reduced frequency of cell death. *A*: Insulin secretion from isolated, perifused islets in response to low/high glucose and KCl. *B*: Glucagon suppression during the same experiment performed in *A*. *C*: Relative β-cell volume (islet area/pancreas area) determined from histologic analysis of pancreata. *D*: Islet number corrected by pancreas area. *E*: Frequency of β-cell proliferation determined as the number of Ki67/insulin-positive cells per relative islet area. *F*: Frequency of β-cell death was calculated as the number of TUNEL/insulin-positive cells per relative islet area. *G*: Representative images of histologic samples used for calculations in *C*–*E*. Pancreata stained as follows: *panel 1*, hematoxylin and eosin (H&E) stain; *panel 2*, insulin stain; *panel 3*, Ki-67 stain. Arrow denotes a Ki-67– positive cell; *panel 4*, TUNEL/insulin costain. Arrow denotes a TUNEL/insulin-positive cell. H&E viewed at original magnification ×40, all others at ×100. *n* = 3–7 per group. Data were analyzed by Student *t* test. *P < 0.05. Data represent the mean ± SEM. (A high-quality digital representation of this figure is available in the online issue.)

be more a function of increased islet size rather than number ($P = 0.22$; Fig. 4*D*). There was no difference in the frequency of Ki-67–positive β-cells between genotypes (Fig. 4*E* and *G*), suggesting that β-cell proliferation rates were not increased in the *db/db*-SGLT2$^{-/-}$ mice. However, the frequency of TUNEL-positive β-cells was 64% less in *db/db*-SGLT2$^{-/-}$ mice (Fig. 4*F* and *G*), indicating that rates of cell death were slower. Thus, improvements in β-cell function observed in vivo appeared to result from maintained β-cell mass due to reduced frequency of β-cell death.

DISCUSSION

Type 2 diabetes is characterized by impaired glucose-stimulated insulin secretion, which is strongly associated with hyperglycemia in rodent and human studies (8,9, 11,26). Chronic hyperglycemia may shift the balance of β-cell proliferation and apoptosis toward cell death, resulting in β-cell deficiency and impaired insulin secretion (8,10,27). Although there seem to be some differences between rodents and humans with regard to the importance of

β-cell proliferation in response to hyperglycemia, human autopsy studies have demonstrated a decline in β-cell mass in individuals with type 2 diabetes that was associated with increased β-cell death (9). A major finding of our study was that reducing glucose toxicity in a model of extreme diabetes preserved islet mass and improved insulin secretion in vivo. Increasing renal glucose excretion in *db/db* mice by SGLT2 deletion produced beneficial effects in glucose homeostasis and, importantly, islet function.

The lack of difference in islet function during isolation/ perifusion studies described here suggested that the primary mechanism by which reduced glucose toxicity improved glucose-stimulated insulin secretion was through preservation of islet mass rather than a change in individual β-cell function. A similar effect was observed after pharmacologic inhibition of SGLT2 in *db/db* and KK-A^{y} mice for 12 and 9 weeks, where total pancreatic insulin content and immunohistologic staining for insulin were increased in treated mice (16,28). No human studies with SGLT2 inhibitors have addressed islet function directly, and so the potential for SGLT2 inhibition to preserve β-cell

mass by reducing glucose toxicity, as it did here in rodents, remains to be determined.

Hyperglycemia in insulin-resistant or -deficient models has also been shown to contribute to peripheral insulin resistance (12,29). Despite a 64% increase in the GIR required to maintain euglycemia in db/db-SGLT2$^{-/-}$ mice, equivalent improvements in measured indices of insulin sensitivity were not detected during euglycemic clamps. There was no difference in whole-body or tissue-specific glucose uptake, and endogenous glucose production was modestly improved by 24% in db/db-SGLT2$^{-/-}$ mice. It seems likely that unaccounted for differences in GIR could result from glucosuria, but estimating acute glucosuria during the clamp was technically difficult. Furthermore, db/db mice possess a complex metabolic phenotype and insulin resistance stemming from multiple factors, including hyperglycemia, hyperlipidemia, and hypercorticosteronemia (30–32). An even modest improvement in insulin resistance in this model suggests that reducing glucose toxicity by renal glucose excretion may produce even more beneficial effects on insulin resistance under less severe circumstances. In fact, inhibition of SGLT2 in ZDF rats for 15 days improved insulin sensitivity (15).

In contrast to the subtle improvement in insulin sensitivity, SGLT2 knockout markedly improved glucose intolerance under HFD-induced, insulin-resistant conditions, and reduced fasting plasma glucose and insulin levels. RC/SGLT2$^{-/-}$ mice also displayed improved glucose tolerance and reduced fasting plasma glucose, without hypoglycemia. Interestingly, SGLT2 knockout resulted in substantially increased caloric intake. Whether this was a response to mild, undetected hypoglycemia or for other reasons remains to be determined. Of note, SGLT2 mutations in humans that result in familial renal glucosuria rarely cause hypoglycemia (33–35). Likewise, the incidence of hypoglycemia during clinical trials of SGLT2 inhibitors is extremely low (17–22).

Inhibition of SGLT2 has the potential to promote negative energy balance and, in turn, weight loss. The lack of differences in plasma electrolytes, phosphate, BUN, creatinine, and the BUN/creatinine ratio suggested that volume depletion did not account for the differences in body weight. Lack of volume depletion in SGLT2$^{-/-}$ mice was also noted in a recent study; however, no difference in body weight was detected (6). Mice in the previous report were studied at between 12 and 20 weeks of age, and group sizes for the body weight data ranged from 6 to 10. Here, mice were studied at 16 weeks, and the group size for body weight data were 16 per group. The breadth of ages cited in the previous report, as well as smaller group sizes, may account for the discrepancy. In support of reduced body weight with loss of SGLT2 function, a recently described SGLT2 mutant mouse with glucosuria similar to that described here was also noted to have reduced body weight (36).

In fact, evidence from the literature supports the notion of reduced body weight with SGLT2 deletion. Short-term studies of approximately 2 weeks have demonstrated no effect of SGLT2 inhibition on body weight in ZDF rats (14,15), whereas longer-term studies of 8 weeks or more have found reductions in body weight in rodents and humans (13,16,19–21). Glucosuria that produced weight loss in humans ranged from 50 to 80 g/day, or 10–16% of a 2,000 kcal/day diet (19,20). In SGLT2$^{-/-}$ mice, glucosuria averaged 0.48 mg/day or 13% of the daily caloric intake of WT mice in this study. Interestingly, feeding increased

about 20% in SGLT2$^{-/-}$ mice, suggesting that an isocaloric diet would have a greater potential for weight loss during SGLT2 deficiency. Previous studies in rodents have also noted concomitant increases in feeding behavior and weight loss during SGLT2 inhibition (13,16). Although RC/SGLT2$^{-/-}$ mice weighed 10% less than RC/WT mice, there was no significant difference in body weight after 4 weeks HFD, although SGLT2$^{-/-}$ mice weighed about 6% less. RC and HFD mice both had increased urine production during periods of food intake, and there was overall less urine output and glucosuria on the HFD compared with RC. Together, these data suggest that SGLT2 activity is greatest in the postprandial setting and that inhibition will produce greater weight loss on a carbohydrate-rich diet.

In conclusion, SGLT2 deletion in mice resulted in profound glucosuria and compensatory behavioral adaptations aimed at replacing water and calories lost in the urine. SGLT2 knockout led to favorable reductions in plasma glucose and insulin during HFD and in the context of genetic obesity. Perhaps the most ominous complication of diabetes is loss of islet function, because this will accelerate the deterioration of glucose homeostasis and increase the exposure to glucose toxicity. Ablation of SGLT2 in db/db mice prevented loss of β-cell mass and thus preserved in vivo glucose-stimulated insulin secretion, which partly accounted for the overall improvements in glucose homeostasis. Taken together, these data support SGLT2 inhibition as a viable insulin-independent treatment for type 2 diabetes.

REFERENCES

1. Chao EC, Henry RR. SGLT2 inhibition—a novel strategy for diabetes treatment. Nat Rev Drug Discov 2010;9:551–559
2. Nair S, Wilding JP. Sodium glucose cotransporter 2 inhibitors as a new treatment for diabetes mellitus. J Clin Endocrinol Metab 2010;95:34–42
3. Wright EM, Turk E. The sodium/glucose cotransport family SLC5. Pflugers Arch 2004;447:510–518
4. Pajor AM, Hirayama BA, Wright EM. Molecular evidence for two renal Na+/glucose cotransporters. Biochim Biophys Acta 1992;1106:216–220
5. Kanai Y, Lee WS, You G, Brown D, Hediger MA. The human kidney low affinity Na+/glucose cotransporter SGLT2. Delineation of the major renal reabsorptive mechanism for D-glucose. J Clin Invest 1994;93:397–404
6. Vallon V, Platt KA, Cunard R, et al. SGLT2 mediates glucose reabsorption in the early proximal tubule. J Am Soc Nephrol 2011;22:104–112
7. Saltiel AR. New perspectives into the molecular pathogenesis and treatment of type 2 diabetes. Cell 2001;104:517–529
8. Federici M, Hribal M, Perego L, et al. High glucose causes apoptosis in cultured human pancreatic islets of Langerhans: a potential role for regulation of specific Bcl family genes toward an apoptotic cell death program. Diabetes 2001;50:1290–1301

9. Butler AE, Janson J, Bonner-Weir S, Ritzel R, Rizza RA, Butler PC. Beta-cell deficit and increased beta-cell apoptosis in humans with type 2 diabetes. Diabetes 2003;52:102–110

10. Donath MY, Gross DJ, Cerasi E, Kaiser N. Hyperglycemia-induced beta-cell apoptosis in pancreatic islets of Psammomys obesus during development of diabetes. Diabetes 1999;48:738–744

11. Rossetti L, Shulman GI, Zawalich W, DeFronzo RA. Effect of chronic hyperglycemia on in vivo insulin secretion in partially pancreatectomized rats. J Clin Invest 1987;80:1037–1044

12. Rossetti L, Smith D, Shulman GI, Papachristou D, DeFronzo RA. Correction of hyperglycemia with phlorizin normalizes tissue sensitivity to insulin in diabetic rats. J Clin Invest 1987;79:1510–1515

13. Fujimori Y, Katsuno K, Nakashima I, Ishikawa-Takemura Y, Fujikura H, Isaji M. Remogliflozin etabonate, in a novel category of selective low-affinity sodium glucose cotransporter (SGLT2) inhibitors, exhibits antidiabetic efficacy in rodent models. J Pharmacol Exp Ther 2008;327:268–276

14. Fujimori Y, Katsuno K, Ojima K, et al. Sergliflozin etabonate, a selective SGLT2 inhibitor, improves glycemic control in streptozotocin-induced diabetic rats and Zucker fatty rats. Eur J Pharmacol 2009;609:148–154

15. Han S, Hagan DL, Taylor JR, et al. Dapagliflozin, a selective SGLT2 inhibitor, improves glucose homeostasis in normal and diabetic rats. Diabetes 2008;57:1723–1729

16. Katsuno K, Fujimori Y, Ishikawa-Takemura Y, Isaji M. Long-term treatment with sergliflozin etabonate improves disturbed glucose metabolism in KK-A(y) mice. Eur J Pharmacol 2009;618:98–104

17. Komoroski B, Vachharajani N, Boulton D, et al. Dapagliflozin, a novel SGLT2 inhibitor, induces dose-dependent glucosuria in healthy subjects. Clin Pharmacol Ther 2009;85:520–526

18. Komoroski B, Vachharajani N, Feng Y, Li L, Kornhauser D, Pfister M. Dapagliflozin, a novel, selective SGLT2 inhibitor, improved glycemic control over 2 weeks in patients with type 2 diabetes mellitus. Clin Pharmacol Ther 2009;85:513–519

19. List JF, Woo V, Morales E, Tang W, Fiedorek FT. Sodium-glucose cotransport inhibition with dapagliflozin in type 2 diabetes. Diabetes Care 2009;32:650–657

20. Wilding JP, Norwood P, T'joen C, Bastien A, List JF, Fiedorek FT. A study of dapagliflozin in patients with type 2 diabetes receiving high doses of insulin plus insulin sensitizers: applicability of a novel insulin-independent treatment. Diabetes Care 2009;32:1656–1662

21. Bailey CJ, Gross JL, Pieters A, Bastien A, List JF. Effect of dapagliflozin in patients with type 2 diabetes who have inadequate glycaemic control with metformin: a randomised, double-blind, placebo-controlled trial. Lancet 2010;375:2223–2233

22. Ferrannini E, Ramos SJ, Salsali A, Tang W, List JF. Dapagliflozin monotherapy in type 2 diabetic patients with inadequate glycemic control by diet and exercise: a randomized, double-blind, placebo-controlled, phase 3 trial. Diabetes Care 2010;33:2217–2224

23. Choi CS, Savage DB, Abu-Elheiga L, et al. Continuous fat oxidation in acetyl-CoA carboxylase 2 knockout mice increases total energy expenditure, reduces fat mass, and improves insulin sensitivity. Proc Natl Acad Sci USA 2007;104:16480–16485

24. Pongratz RL, Kibbey RG, Kirkpatrick CL, et al. Mitochondrial dysfunction contributes to impaired insulin secretion in INS-1 cells with dominant-negative mutations of HNF-1alpha and in HNF-1alpha-deficient islets. J Biol Chem 2009;284:16808–16821

25. Jurczak MJ, Danos AM, Rehrmann VR, Allison MB, Greenberg CC, Brady MJ. Transgenic overexpression of protein targeting to glycogen markedly increases adipocytic glycogen storage in mice. Am J Physiol Endocrinol Metab 2007;292:E952–E963

26. Bonner-Weir S, Trent DF, Weir GC. Partial pancreatectomy in the rat and subsequent defect in glucose-induced insulin release. J Clin Invest 1983;71:1544–1553

27. Finegood DT, McArthur MD, Kojwang D, et al. Beta-cell mass dynamics in Zucker diabetic fatty rats. Rosiglitazone prevents the rise in net cell death. Diabetes 2001;50:1021–1029

28. Arakawa K, Ishihara T, Oku A, et al. Improved diabetic syndrome in C57BL/KsJ-db/db mice by oral administration of the Na(+)-glucose cotransporter inhibitor T-1095. Br J Pharmacol 2001;132:578–586

29. Unger RH, Grundy S. Hyperglycaemia as an inducer as well as a consequence of impaired islet cell function and insulin resistance: implications for the management of diabetes. Diabetologia 1985;28:119–121

30. Kahn BB, Flier JS. Obesity and insulin resistance. J Clin Invest 2000;106:473–481

31. Zinker B, Mika A, Nguyen P, et al. Liver-selective glucocorticoid receptor antagonism decreases glucose production and increases glucose disposal, ameliorating insulin resistance. Metabolism 2007;56:380–387

32. Gibbs EM, Stock JL, McCoid SC, et al. Glycemic improvement in diabetic db/db mice by overexpression of the human insulin-regulatable glucose transporter (GLUT4). J Clin Invest 1995;95:1512–1518

33. Santer R, Kinner M, Lassen CL, et al. Molecular analysis of the SGLT2 gene in patients with renal glucosuria. J Am Soc Nephrol 2003;14:2873–2882

34. Calado J, Sznajer Y, Metzger D, et al. Twenty-one additional cases of familial renal glucosuria: absence of genetic heterogeneity, high prevalence of private mutations and further evidence of volume depletion. Nephrol Dial Transplant 2008;23:3874–3879

35. Francis J, Zhang J, Farhi A, Carey H, Geller DS. A novel SGLT2 mutation in a patient with autosomal recessive renal glucosuria. Nephrol Dial Transplant 2004;19:2893–2895

36. Ly JP, Onay T, Sison K, Sivaskandarajah G, et al. Sweet Pee model for Sglt2 mutation. J Am Soc Nephrol 2011;22:113–123